View metadata, citation and similar papers at core.ac.uk
brought to you by CORE
provided by JKI Open Journal Systems (Julius Kühn-Institut)



# 04-05: ATR-FTIR imaging reveals cell wall layer-specific chemotypes in poplar tension wood

Clément Cuello[1,2], Paul Marchand[1], Françoise Laurans[1,3], Camille Grand-Perret[1], Véronique Lainé-Prade[1,3], Gilles Pilate[1], Annabelle Déjardin[1]

*[1]UMR BioForA, INRA, ONF, F-45075 Orléans Cedex 2, France*
*[2]Ecole Doctorale 549 SSBCV, Université d'Orléans, F-45067 Orléans Cedex 2, France*
*[3]Plateforme régionale Génobois, F-45075 Orléans Cedex 2, France*
*E-mail: clement.cuello@inra.fr*

Trees are able to grow high and live old thanks to the remarkable properties of their wood. Indeed, wood delivers three major functions: (1) water conduction from roots to crown, (2) mechanical support of the ever-increasing mass of the growing tree and (3) storage of temporary reserves, important for tree growth over the years. In angiosperm trees, vessels, fibers and parenchyma rays are respectively assigned to each of these functions [1]. Fibers are characterized by a thick secondary cell wall, made of several S-layers. Cell wall structure and composition strongly vary according to developmental stages and environmental conditions. For example, in response to mechanical constraints, angiosperm trees produce tension wood (TW) whose fibers exhibit a thick gelatinous extra-layer, named G-layer (Fig.1A-B). This layer, located in place of the usual S2 and/or S3 layers, consists mainly of cellulose and non-cellulosic polysaccharides with nearly no lignin [2,3]. By contrast, opposite wood (OW) located on the opposite side of the trunk is totally deprived of fibers with G-layers (Fig.1C). Hence, the high complexity of wood may stand as a hindrance for studying its formation and the construction of its properties. However, this can be circumvented thanks to the development of cell-specific approaches and microphenotyping.

Here, we report the development of a non-destructive microphenotyping method based on ATR-FTIR imaging. We applied this technique on stem cross sections of poplars (INRA 717-1B4, *Populus tremula* x *P. alba*) which were tilted to induce the production of TW. Hyperspectral images were acquired using Spectrum 400 FTIR spectrophotometer coupled to a Spotlight 300 FTIR imaging system (PERKIN ELMER, Wellesley, USA). Three 100 x 100µm images per cross-section were taken at a 1.56 x 1.56µm pixel dimension. This high spatial resolution was made possible by the use of a high refractive index crystal. Thus, we were able to clearly distinguish the different cells (Fig.1D-E). ATR-FTIR spectra were also acquired on powders from i) ground stems, ii) enriched in TW or iii) in OW, and iv) on isolated G-layers.

We performed several pre-treatments on the 4 $cm^{-1}$-resolution spectra: background correction during acquisition, noise reduction, atmospheric correction, Savitzky-Golay smoothing, SNV normalization and first derivation. We then applied diverse unsupervised multivariate image analyses such as principal component analysis, hierarchical clustering on principal component and multiple curve resolution, leading to clusters of pixels representative of one chemotype (Fig.1F-G). Non parametric analysis allowed us to identify significant differences of absorbance between those chemotypes. We demonstrated that spectra taken from fiber cell walls on cross-sections differed from spectra obtained from wood powder. Interestingly, spectra from isolated G-layer were very closely related to those obtained through ATR-FTIR microspectroscopy of G-layers on cross-sections (1.H). We also showed that ATR-FTIR imaging was able to discriminate between fiber, vessel and ray cell walls. These findings are in accordance with previous studies [4,5] but with a five-fold increased spatial resolution.

Peak assignments based on the literature made possible to give some biological consistence to our observations. We showed that (i) G-layers were mainly composed of cellulose and non-cellulosic polysaccharides, (ii) lignins in rays cell walls were mainly G-units whereas

lignins from fiber cell walls were mainly S-units (Fig.1I). These findings are in accordance with previous studies [3-6].

In a nutshell, ATR-FTIR microspectroscopy brings new opportunities for the study of cell wall composition at the cell level and appears to be a promising tool to finely characterize the cell wall of different wood cell types.

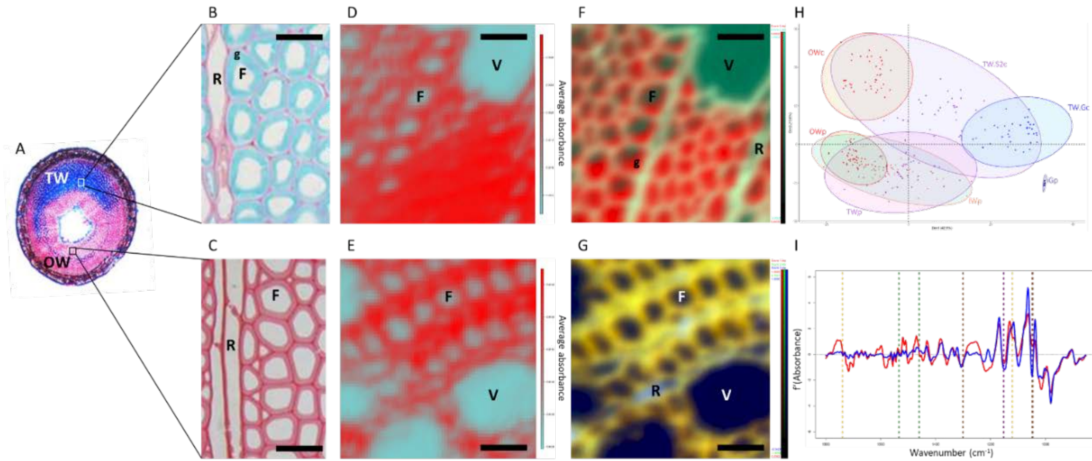


Fig. 1. Toward the identification of discriminant wavenumbers. Cross section of tilted poplar stem (**A**), TW (**B**) and OW (**C**) after safranine/astra blue staining. Raw Infra-red images of TW (**D**) and OW (**E**). PCA reconstructed images of TW (**F**) and OW (**G**). PCA discriminating the spectra of the different types of walls (**H**). First derived and SNV standardized mean spectra of OW (red) and TW (blue) (**I**).

Global: OW: opposed wood; TW: tension wood; g: G-layer, R: rays, F: fiber, V: vessel, Scale bars: 10 µm. PCA: Score: score of the main components, Red: OW spectra (Owc, Owp), dark blue: isolated G layer spectra (iGp), blue: G layer spectra on cross-sections (TW.Gc), purple: S2-layer spectrum of TW (TW.S2c) and TW powder (TWp), pale pink: tilted stem spectra (TSp), square: spectra acquired on cross-sections (Owc, TW.Gc, TW.S1c), round: spectra acquired on powders (Owp, TWp, TSp, iGp). Each point represents a spectrum The ellipses represent 99% of the spectra if they follow a normal distribution. Before analysis, the spectra were first derived and normalized by SNV. Spectra: Dotted: differentially absorbed wave numbers, Green: lignins, Yellow: cellulose, Brown: hemicelluloses, Violet: pectins.

**References**

[1] DÉJARDIN, A., et al., 2010: C R Biol, **333**, 325-334.

[2] PILATE, G., et al., 2004: New Phytologist, **164**, 63–72.

[3] GUEDES, F.T.P., et al., 2017: Planta, **246**, 857–878.

[4] OLSSON, A.M., et al., 2011: Planta, **233**, 1277–1286.

[5] GORZSÁS, A., et al., 2011: Plant Journal, **66**, 903–914.

[6] TERASHIMA, N., and K. FUKUSHIMA, 1993: In Forage Cell Wall Structure and Digestibility, Chap, **10**, 247-270.